A boundary-layer study near Ross Island using acoustic remote sensing

ZHONG LIU, JERRY K. GEER, *and* DAVID H. BROMWICH

Byrd Polar Research Center
Ohio State University
Columbus, Ohio 43210

Planetary boundary-layer studies in Antarctica have improved greatly since the introduction of automatic weather station data and satellite images. Due to the height limitation of automatic weather station data, however, such boundary-layer studies are restricted to phenomena which have a surface expression (Neff 1981; Mastrantonio, Ocone, and Fiocco 1988). A sodar (an abbreviation for *sonic detection and ranging*) can overcome this limitation by providing three-dimensional wind and backscatter data up to an altitude of several hundred meters. During the 1990 campaign, we used a sodar at Williams Field (figure 1), a place on the Ross Ice Shelf near the southwestern tip of Ross Island strongly influenced by the surrounding complex topography and by the mesoscale and synoptic-scale pressure systems. The main purposes of the campaign were to test out the sodar in the harsh antarctic environment and to gain further understanding of the characteristics and evolution of the boundary layer in such a complex setting.

The sodar used in this campaign is of a special configuration designed by Radian Corporation especially for operations in Antarctica (temperatures ranged from −32 °C to +3 °C and wind speeds up to 18 meters per second were experienced). The unit is compact relative to the most common sodar designs and is constructed of durable, light-weight materials. It is also mounted on skis for portability.

The fundamental principle of the sodar is quite straightforward, though it is possible to employ fairly rigorous signal-processing techniques. The three-axis, monostatic sodar is composed of three acoustic transducers mounted at the focal points of three parabolic reflectors. These assemblies are each enclosed in a protective fiberglass cylinder which has a layer of acoustic dampening foam on its inside surface. Each one of these three shielded transceivers constitutes what the designers refer to as a *leg*.

These legs are mounted in line on a rack at specific orientations. The center leg lies along the vertical axis. The next leg lies in the plane formed by the vertical axis and the long axis of the rack but is oriented at an angle of 22.5 degrees away from vertical. The last leg is also tilted at an angle of 22.5 degrees but in a plane normal to the plane containing the axes of the other two legs.

This particular sodar operates at an acoustic frequency of 2250 hertz. The sodar collects data by transmitting a 2250-hertz pulse of selected duration in a round-robin fashion from each of the legs. Immediately following the transmission of a pulse from one leg, the same transducer switches to receiving mode. Based on the known frequency, pulse duration, and leg orientation, a specialized signal-processing card located in a microcomputer expansion slot calculates the three dimensional wind values and passes them to the computer to be written to disk for subsequent analysis.

The 1990 campaign lasted from 19 October to 5 November. During this period, we experienced a significant diurnal variation of the boundary layer under the influence of insolation. In figure 2, the average 3-hour surface air temperatures over this period show a maximum at 1200 local time and a minimum at 0000 local time, respectively. The effect of surface heating over the ice shelf also extends to a certain height. Intermittent balloon sounding data show that the vertical temperature profile on a typical day, which has some clouds around, evolves in the following three stages. In stage I, the ground-based inversion layer is raised aloft as the insolation increases. The maximum height rise did not exceed 200 meters during the campaign. In stage II, the elevated inversion descends following from the decrease of absorbed solar energy and gradually in-

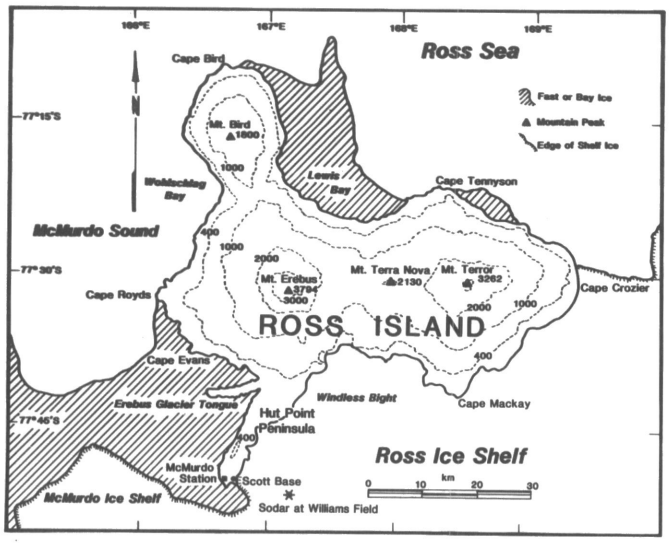

Figure 1. Topographic map of Ross Island, adapted from O'Connor and Bromwich (1988). The sodar was located at Williams Field. (km denotes kilometer.)

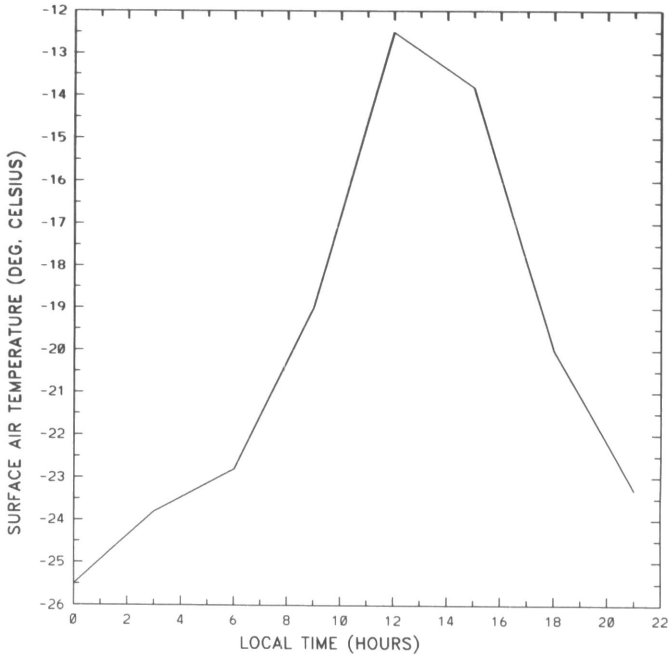

Figure 2. Average surface air temperature based on 3-hour observations from 19 October to 6 November 1990.

creasing net heat loss from longwave radiation. In stage III, strong net heat loss from longwave radiation strengthens and reconstructs the ground-based inversion layer. Hourly mean resultant wind speed profiles derived from the sodar data follow this diurnal change under 500-meter height with maxima being found after midday and minima after midnight.

Studies of the blocking effect of Ross Island on stratified near-surface air have been reported by Schwerdtfeger (1984), Slotten and Stearns (1987), and O'Connor and Bromwich (1988). The 24-hour average resultant wind direction profile below 500 meters altitude from the sodar records (figure 3*A*, solid line) shows the following:

- a large wind direction deviation from the mean flow at low levels due to the island deflection and the blocking effect of Hut Point Peninsula up to 200 meters altitude;
- a gradual clockwise decrease of this deviation as the height increases;
- unidirectional airflow above 326 meters.

Figure 3*B*, plotted from sodar horizontal wind records, shows an example of the island blocking effect. The clockwise wind directional rotation starts from the bottom level (northeast wind) and ends up with a uniform wind direction (southeast wind) above 300 meters altitude.

Strong sodar backscatter obtained during the campaign was found to have a close relation with wind-shear magnitudes. According to the acoustic scattering cross-section equation (Batchelor 1957; Tatarskii 1971), received sodar backscatter signals are proportional to spatial temperature inhomogeneities. Analysis of backscatter and wind-shear magnitudes supports the idea that wind-shear magnitudes may be the key factor for generation of temperature inhomogeneities. The wind shears that appeared during the campaign are classified as follows:

- strong wind speed shear;
- wind direction shear accompanying strong wind speed;
- both wind speed and direction shears.

Thermal convection is not a major contributor to generation of sodar backscatter in this area during spring.

Three-dimensional sodar wind data provide a variety of information on the structure of the boundary layer. The 24-hour average resultant wind speed profile (figure 3*A*, dashed line) shows a maximum wind speed at 75 meters, a feature that may be classified as a low-level jet (Stull 1988). The hourly average resultant wind speed profiles show the evolution of this jet, which becomes less well-defined at midday and midnight.

In conclusion, the sodar deployment at Williams Field during the 1990 campaign was successful, and it proved to be an effective tool for probing the behavior of the stable planetary layer. An extensive field study of the katabatic winds near Siple Coast using a combination of a sodar and a RASS (radio acoustic sounding system for sensing the temperature profile) at each of two camps is planned for all of November 1991.

This research was supported by National Science Foundation grant DPP 89-16921 to David H. Bromwich.

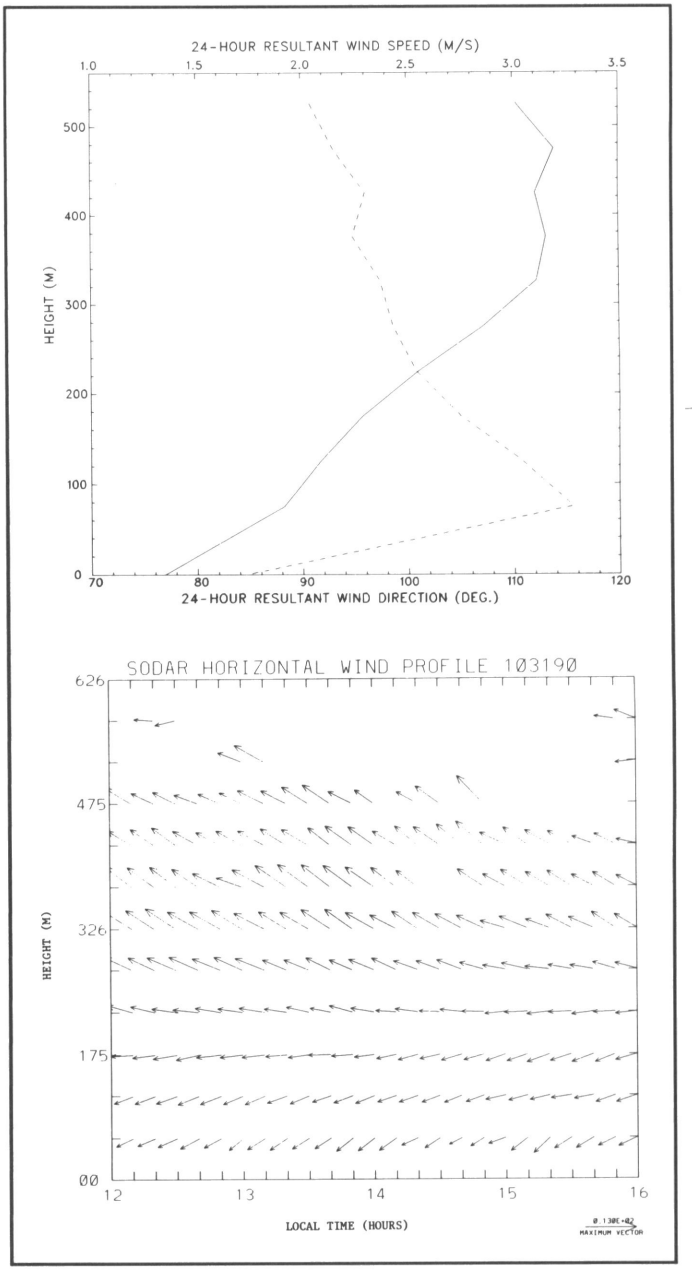

Figure 3. *A.* 24-hour resultant wind derived from sodar horizontal wind records during the campaign. Solid line: 24-hour resultant wind direction versus height. A clockwise rotation of wind direction results from the blocking effect of Hut Point Peninsula and Ross Island. Dashed line: 24-hour resultant wind speed versus height. A wind speed maximum is located at 75 meters altitude. (M denotes meter. M/S denotes meters per second.) *B.* An example of the blocking effect from 1200 to 1600 local time, 31 October 1990. The vector length gives wind speed in meters per second, and the orientation shows the wind direction with an easterly moving from right to left. (M denotes meter.)

References

Batchelor, G.K. 1957. Wave scattering due to turbulence. In F.S. Sherman (Ed.), *Symposium on Naval Hydrodynamics NAS-NRC* (Publication number 515). Washington, D.C.: National Research Council.

Mastrantonio, G., R. Ocone, and G. Fiocco. 1988. Acoustic remote sensing of the Antarctic boundary layer. In M. Colacino, G. Giovannelli and L. Stefanutti (Eds.), *Italian research on Antarctic atmosphere conference proceedings* (Vol. 20). Bologna, Italy: Italian Physical Society.

Neff, W.D. 1981. *An observational and numerical study of the atmospheric boundary layer overlying the East Antarctic Ice Sheet.* (NOAA Technical Memorandum ERL WPL-67). Boulder, Colorado: National Oceanic and Atmospheric Administration.

O'Connor, W.P., and D.H. Bromwich. 1988. Surface airflow around Windless Bight, Ross Island, Antarctica. *Quarterly Journal of the Royal Meteorological Society,* 114, 917–938.

Schwerdtfeger, W. 1984. *Weather and climate of the Antarctic.* New York: Elsevier Science Publishers.

Slotten, H.R., and C.R. Stearns. 1987. Observations of the dynamics and kinematics of the atmospheric surface layer on the Ross Ice Shelf, Antarctica. *Journal of Climate and Applied Meteorology,* 26, 1731–1743.

Stull, R.B. 1988. *An introduction to boundary layer meteorology.* Boston: Kluwer Academic Publishers.

Tatarskii, V.I. 1971. *The effects of the turbulent atmosphere on wave propagation.* (Israel Program for Scientific Translations.) Washington, D.C.: U.S. Department of Commerce.

Real-time, *in situ* measurement of hydrogen chloride and sulfur dioxide in the plume of Mount Erebus

William D. Bowers *and* Raymond L. Chuan

Femtometrics
Costa Mesa, California 92627

Philip R. Kyle

Department of Geoscience
New Mexico Institute of Mining and Technology
Socorro, New Mexico 87801

The only significant source of gases and aerosols in the antarctic atmosphere is Mount Erebus, the southernmost active volcano. Using a multistage quartz crystal microbalance cascade impactor, research teams have measured emissions at the rim of Mount Erebus and throughout the continent to determine the impact Mount Erebus has on Antarctica (Chuan 1976, Chuan et al. 1986; Meeker, Kyle, and Chuan 1985). The gaseous makeup of the Mount Erebus plume has also been measured by several methods (Stoiber, Malincomico, and Williams 1983; Rose, Chuan, and Kyle 1983; Crowe et al. 1987; Finnegan et al. 1989). Previously, however, hydrogen chloride and sulfur dioxide concentrations emitted by Mount Erebus have not been directly determined. We report here real-time, *in situ* measurements of hydrogen chloride and sulfur dioxide gases in the Mount Erebus plume. The measurements were made using a modified quartz crystal microbalance cascade impactor.

The quartz crystal microbalance cascade impactor has been the primary instrument used to measure the size distribution and mass concentration of aerosols in the antarctic atmosphere. The ambient aerosols, segregated by their size, are collected when they impact a piezoelectric crystal, which serves as sensitive mass balance. A piezoelectric crystal operates as a mass microbalance by measuring the change in its oscillating frequency due to a change in mass on the surface of the crystal. When a carefully chosen chemical coating is applied to the crystal's surface, the crystal becomes a selective and highly sensitive chemical vapor sensor (Karmarker and Guilbault 1974; Cooke, West, and Watts 1980). The crystal coating must have a selective and specific response to the gas of interest but must not respond to other, interferring gases present.

For our work, the crystal was coated with triethanolamine (TEA), a substance which responds to both hydrogen chloride and sulfur dioxide. The detection concept is illustrated in figure 1. The response due to a 1-minute, 12-parts-per-million sulfur dioxide exposure is shown in figure 1*A*. During the exposure, the sulfur dioxide diffuses into the TEA, increasing the mass of material on the crystal. This is seen as an increase in the sensor signal. After the 1-minute exposure, the sulfur dioxide TEA diffuses, and the signal returns to baseline as the mass on the crystal decreases. A 449-hertz response was observed for

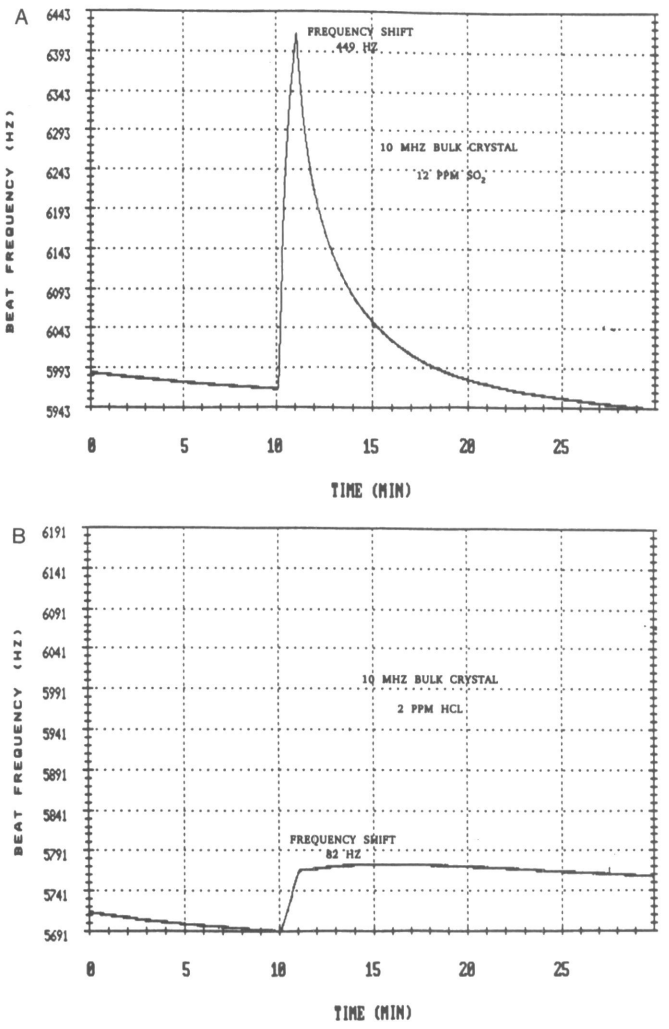

Figure 1. Example of chemical vapor detection using piezoelectric crystal coated with triethanolamine. *A.* Response due to a 1-minute exposure to 12 parts per million (ppm) of sulfur dioxide (SO_2) at the 10-minute mark. This is a reversible interaction. *B.* Response due to a 1-minute exposure to 2 parts per million of hydrogen chloride (HCl) at the 10-minute mark. This is an irreversible interaction. (HZ denotes hertz; MHZ denotes megahertz.)